Impact of steel properties on the susceptibility to corrosion of weld mesh and mesh straps

by J. Hadjigeorgiou, S.J. Thorpe, E. Storimans, and F.D. Agrensa

Affiliation:
University of Toronto, Canada

Correspondence to:
J. Hadjigeorgiou

Email:
john.hadjigeorgiou@utoronto.ca

ORCID:
J. Hadjigeorgiou
http://orcid.org/0000-0002-6047-3964

Abstract

Reinforcement and surface support are part of an integrated system that transfers and shares load until the excavation surface is stabilized or until the ground support system fails. Steel mesh is the most popular primary surface support element in underground hard rock mines in Canada. Mesh straps are a secondary surface support that provide additional containment as they distribute the load between and across the reinforcement elements.

This investigation addresses the role of steel properties, and in particular steel chemistry, in the long-term performance of mesh and mesh straps when exposed to an aggressive corrosive environment. It reports on comparative accelerated corrosion studies to compare the resistance to corrosion of different surface support elements. This has significant implications on the choice of surface support and the anticipated rehabilitation requirements.

Keywords

accelerated corrosion of ground support, primary and secondary surface support, steel properties

Introduction

A ground support system employs both reinforcement and surface support elements to maintain the integrity of an excavation in hard rock for its intended working life. Although there are multiple reinforcement elements in use, including conventional and energy-absorbing rockbolts, the main surface support options are shotcrete and mesh.

Steel mesh is the most popular surface support element in underground hard rock mines in Canada to hold and retain the fractured rock between the reinforcement elements under both static and dynamic loading conditions. Mesh straps are often used as a secondary support over mesh or shotcrete, to contain the rock mass and distribute the load between the reinforcement elements.

In practice, mesh is often the weakest link in a ground support system (Simser, 2008). Hadjigeorgiou and Stacey (2018) noted that mesh can fail as a result of multiple factors that include installation related issues (e.g., mesh opening due to inadequate overlap, or rockbolt plates cutting through the screen), damage (e.g., due to flyrock following blasting, or equipment that caused damage), and the inability of the mesh to meet the static and seismic loads. All these factors affect the long-term performance of mesh and straps that can be further degraded when exposed to an aggressive corrosive environment (Figure 1).

Beyond standard quality assurance and quality control (QA/QC) processes, the traditional focus of investigations of the performance of mesh is on the capacity and deformation of different screen types, e.g., different gauges of weld mesh, (Tannant, 1995). Of additional interest are comparisons between high-tensile strength chain-link and weld mesh, (Player et al., 2008). These laboratory tests provided valuable insight into the anticipated field performance. The limitations of these laboratory studies in extrapolating it to field performance must be fully understood. Baek et al. (2020) used numerical experiments to demonstrate the significant impact of test configuration on the results.

There is limited data on the susceptibility of mesh to corrosion and even less on mesh straps. Hassell et al. (2010) extrapolated the relationship between the reduction in mesh strand diameter due to corrosion and peak load capacity of 1.3 m × 1.3 m mesh sheet. Dorion and Hadjigeorgiou (2014) collected 60 strand samples of #6 (4.9 mm diameter) mesh from Canadian mines exposed to corrosive environments (Figure 3). These were tested to determine the residual tensile strength (or loss in strength) of the wire since installation. Wu et al. (2018) undertook a comparative laboratory study to demonstrate that mesh sheets under 'dry' conditions displayed minimal corrosion effects over 12 weeks, while wet–dry cycle mesh specimens exhibited significant corrosion. Hadjigeorgiou (2016) qualified the influence of corrosion on the capacity of ground support elements to meet the long-term design requirements.

Impact of steel properties on the susceptibility to corrosion of weld mesh and mesh straps
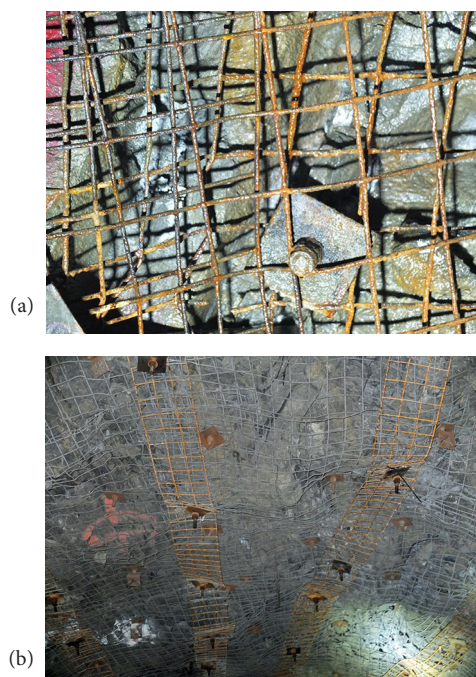

(a)

(b)

Figure 1—(a) Mesh and (b) Straps exposed in a corrosive environment

This paper focuses on the susceptibility of mesh and straps to corrosion with the emphasis on the role of steel properties. This investigation was part of a rigorous QA/QC of an underground mine in Canada where part of its qualification process involved an investigation of two sets of mesh and mesh straps for their susceptibility to corrosion.

Mesh and mesh strap susceptibility to corrosion

It is standard practice that the introduction of a ground support product in underground mines is preceded by a rigorous qualification process. In the case of new ground support elements, this may require a comprehensive qualification process prior to a field trial. In the case of conventional systems, the focus is on compliance with predefined thresholds that are typically focused on meeting capacity and deformation guidelines under laboratory and field conditions. The susceptibility to corrosion is often not part of the process. It has been demonstrated that this can be critical in certain cases when the ground support elements are anticipated to be exposed to potentially corrosive environments.

Long term studies using coupons in an underground mining environment can provide valuable insights on the susceptibility to corrosion of different steel products over time (Figure 2). These tests are, however, both expensive and time consuming to conduct. Accelerated corrosion techniques can provide the relative performance of different ground support elements in a short time. This is important when a decision is to be made on which product to prioritize for field trials. Examples of variations in their susceptibility to corrosion of 'similar' expandable bolts have been provided by Hadjigeorgiou et al. (2020) and for it should read friction rock stabilizers by Hadjigeorgiou et al. (2023)

This paper reports on comparing the influence of steel properties on the susceptibility to corrosion of two sets of mesh and mesh straps from different suppliers. It was part of a due diligence protocol by a mine site aiming to optimize its ground support practice and anticipate the long performance of its primary and secondary support.

Figure 2—Corrosion coupons in a wet environment: (a) on installation, (b) 12 months, Dorion et al. (2010)
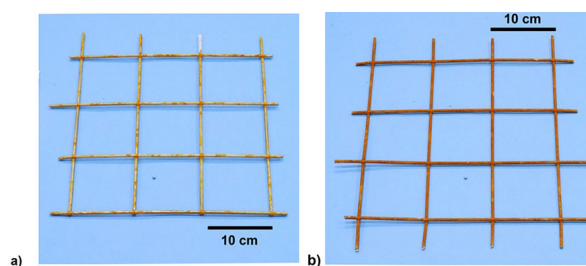

a)

b)

Figure 3—(a) #6 mesh sample from supplier A (M1), (b) #6 mesh sample from supplier B (M2)
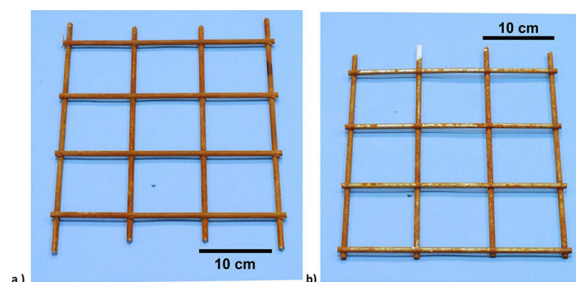

a)

b)

Figure 4—(a) Mesh strap (S1), (b) Mesh strap (S2)

Welded mesh

The mine provided a series of #6 mesh samples typically used as part of its ground support standard to compare their susceptibility to corrosion. For the purposes of this paper, the two #6 mesh products are referred to as M1 and M2 (Figure 3). All samples were received in good condition. None were treated with any corrosion resistant coating, such as galvanization. Of interest was their comparative resistance to corrosion when exposed to the same aggressive environment to anticipate whether their long-term performance would be equivalent.

Mesh straps

Mesh straps are bands of heavy #0-gauge welded mesh, typically available in precut lengths of 1.2 m - 4 m (4-13 ft). They are easy to install because bolts can be fitted at convenient locations through the mesh, (Hadjigeorgiou and Potvin (2012). For the purposes of this investigation, the #0-gauge mesh straps are identified as sample S1 and S2, (Figure 4).

Chemical analysis for mesh and mesh strap products

A chemical analysis based on ASTM E1019-11, 2011 was used for the carbon and sulfur analysis, and inductively coupled plasma atomic emission spectroscopy following the ASTM E1479-16, 2016 procedure was used to determine the concentration of the

Impact of steel properties on the susceptibility to corrosion of weld mesh and mesh straps

remaining elements. The average of three specimens was used for all analyses. Table I summarizes the results of the chemical composition analysis for the #6 M1 and M2 mesh and the S1 and S2 mesh straps.

In general, similar mechanical properties for mesh can be achieved by using different concentrations of chemical alloying elements. Table II describes advantages and limitations of specific elements in the chemical composition of low carbon steel.

Material hardness

For the purposes of this investigation, the hardness of the steel was determined using the Rockwell B hardness test. The test is a measure of the resistance of the material to permanent indentation

and can be used to estimate the tensile strength of the steel. The Rockwell B hardness was determined using a tungsten carbide ball as the indenter with a diameter of 1.588 mm (ASTM E18-22, 2022). Conversion from Rockwell B hardness to approximate tensile strength was made according to ISO 18265:2013. For comparison purposes, the minimum tensile strength, based on the ASTM A1064/1064M-22, 2022 standard is also provided. The results for the mesh are summarized in Table III and for the mesh strap in Table IV.

It is important to note the difference in mechanical properties, between the two mesh, and the mesh strap products. This should be part of the QA/QC process during the manufacturing process and can be compared with additional tensile tests.

Table I

Comparative chemical composition between M1 and M2 mesh and S1 and S2 mesh straps

Element %	Mesh M1 ($\bar{x} \pm \sigma$)	Mesh M2 ($\bar{x} \pm \sigma$)	Mesh Strap S1 ($\bar{x} \pm \sigma$)	Mesh Strap S2 ($\bar{x} \pm \sigma$)
C	0.111 ± 0.006	0.240 ± 0.021	0.188 ± 0.001	0.117 ± 0.001
S	0.011 ± 0.006	0.016 ± 0.002	0.016 ± 0.001	0.004 ± 0.001
Mn	0.443 ± 0.006	0.433 ± 0.012	0.515 ± 0.021	0.457 ± 0.015
P	0.016 ± 0.003	0.026 ± 0.007	0.034 ± 0.002	0.019 ± 0.001
Si	0.183 ± 0.006	0.270 ± 0.035	0.180	0.173 ± 0.006
Cu	0.033 ± 0.006	0.030 ± 0.010	0.01	0.040
Ni	0.017 ± 0.006	0.010 ± 0.000	0.01	0.020
Cr	0.033 ± 0.015	0.023 ± 0.006	0.02	0.033 ± 0.006
V	< 0.01	< 0.01	< 0.01	< 0.01
Mo	< 0.01	0.010 ± 0.000	< 0.01	< 0.01
Al	< 0.01	< 0.01	< 0.01	< 0.01
Co	< 0.01	< 0.01	< 0.01	< 0.01
Ti	< 0.01	< 0.01	< 0.01	< 0.01
Pb	< 0.01	< 0.01	< 0.01	< 0.01

Table II

Advantages and limitations of specific elements in the chemical composition of low carbon steel

Element	Advantages	Limitations
Carbon (C)	Defines the strength and hardness of rockbolts.	Can result in lower ductility, toughness, and machinability.
Sulfur (S)	Increases machinability.	Decreases weldability, impacts toughness and ductility.
Manganese (Mn)	Improves wear resistance and increases strength without reducing forgeability.	
Phosphorus (P)	Results in higher strength and hardness and better machinability.	Results in higher brittleness.
Silicon (Si)	Increases tensile and yield strength, hardness, and forgeability.	
Nickel (Ni)	Increases strength and hardness without sacrificing ductility and toughness.	
Chromium (Cr)	Contributes to increased strength, hardness, toughness, resistance to wear and abrasion, and reduces susceptibility to corrosion.	If combined with carbon, then Cr is not available for corrosion resistance.
Copper (Cu)	Beneficial to the corrosion resistance of steel.	

Table III

Rockwell B hardness and approximate tensile strength for mesh samples M1 and M2

	Mesh M1	Mesh M2
Rockwell B hardness (HRBW)	96.7 ± 1.7	102.2 ± 1.3
Approx. tensile strength (ISO 18265:2013)	740 ± 34 MPa	864 ± 29 MPa
Minimum tensile strength (ASTM A1064/A1064M-22, 2022)	515 MPa	515 MPa

Table IV

Rockwell B hardness and approximate tensile strength for the mesh strap

	Mesh strap S1	Mesh strap S2
Rockwell B hardness (HRBW)	96.7 ± 0.8	89.7 ± 1.5
Approx. tensile strength (ISO 18265:2013)	738 ± 18 MPa	614 ± 23 MPa
Minimum tensile strength (ASTM A1064/A1064M-22, 2022)	515 MPa	515 MPa

Experimental set-up for accelerated corrosion investigations

Accelerated corrosion studies have been used in the past to investigate the susceptibility to corrosion of the steel used in different ground support elements, e.g., expandable rockbolts Hadjigeorgiou et al. (2020), or friction rock stabilizers Hadjigeorgiou et al. (2023). For the purposes of the present investigation, a battery of accelerated corrosion tests was performed to provide a direct comparison between the steel used in the two mesh types and two mesh straps. The objective was to establish if there was a material variation in performance when exposed to an aggressive corrosion environment.

The experimental set-up for open-circuit potential (OCP), linear polarization resistance (LPR), electrochemical impedance spectroscopy (EIS), and potentiodynamic anodic polarization (AP) is provided in Figure 5. A three-electrode cell was used for all experiments. The counter electrode consisted of a platinum mesh and the reference electrode was an Ag/AgCl electrode filled with 3 M KCl. The working electrode was composed of either a mesh or a mesh strap sample. Measured potentials were converted to the saturated calomel electrode scale for reporting. The electrolyte composition is provided in Table V, with the pH adjusted to 2.7 using sulfuric acid.

Open-circuit potential (open cell potential)

The OCP is the potential at which a specimen will equilibrate in a given solution when there is no externally introduced bias applied to the cell. OCP measurements are potentiometric experiments and involve measuring the potential of the material of interest versus a reference electrode with time.

The OCP investigations were conducted in accordance with ASTM G5, and the results are summarized in Figure 6. The OCP for M1 was -0.610 V vs SCE, while the OCP for M2 was -0.621, suggesting that M2 is more susceptible to corrosion than M1 because of its more active open-circuit potential.

An interpretation of the relative performance of the mesh is possible by reference to their chemical composition in Table I. Increased C, P, and Si, content in M2 should decrease the corrosion
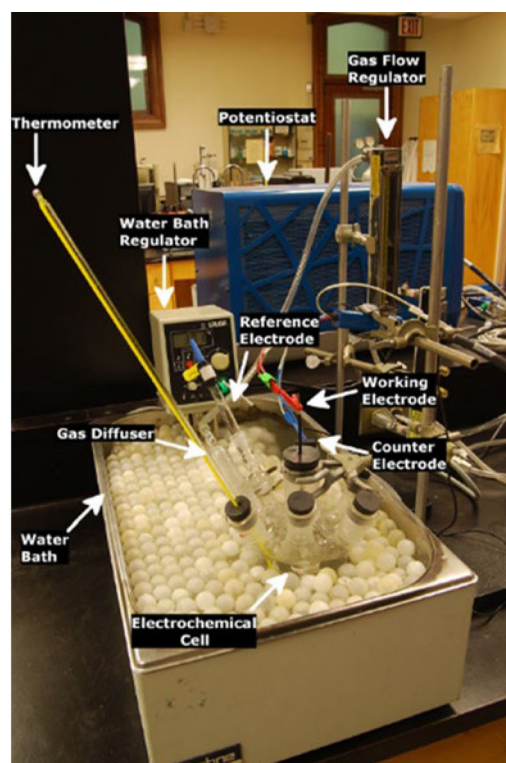

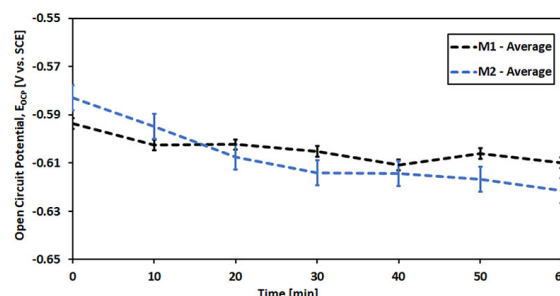**Figure 5—Acceleration corrosion set-up**

Figure 6—Open cell potential comparison for the mesh samples M1 and M2

Table V		
Lixiviate composition (electrolyte) used in accelerated corrosion investigations		
Chemical compound	**Formula**	**g/L**
Magnesium sulfate heptahydrate	$MgSO_4 \cdot 7H_2O$	31.44
Aluminium sulfate octadecahydrate	$Al_2(SO_4)_3 \cdot 18H_2O$	10.49
Zinc sulfate heptahydrate	$ZnSO_4 \cdot 7H_2O$	3.87
Calcium sulfate dihydrate	$CaSO_4 \cdot 2H_2O$	1.76
Ferrous sulfate heptahydrate	$FeSO_4 \cdot 7H_2O$	1.24
Sodium chloride	$NaCl$	0.41
Sodium sulfate anhydrite	Na_2SO_4	0.12

resistance relative to M1. In addition, the slight increases of Cu and Ni content of M1 will improve its corrosion resistance relative to M2.

Linear polarization resistance

LPR is an electrochemical technique used to estimate the corrosion rate near or at the open circuit potential. In this technique, the material is typically biased both anodically and cathodically on the order of ± 10–30 mV relative to the open circuit potential. With the application of said small potential bias in many material–electrolyte systems, this technique can be considered largely non-destructive in nature. The resistance to corrosion can be estimated by taking the slope of the applied potential versus current curve (ASTM G3).

LPR measurements were performed in accordance with ASTM G59-97 (2014). The results are illustrated in Figure 7 and Table VI. It can clearly be seen that M1 has a higher polarization resistance, (R_p), than M2 and is less susceptible to corrosion. This is reflected in the estimated corrosion rates in Table VI which are in agreement with the OCP results that suggest M2 has a higher corrosion rate than M1.

Electrochemical impedance spectroscopy

EIS requires the application of a small (± 5–10 mV) alternating voltage (AC) signal imposed on either the OCP or a given DC bias of a material and measuring the resultant phase shift and amplitude of the current. The frequency response is analyzed to produce an electrical circuit analogue to identify parameters such as solution resistance, interface inductance and capacitance, and charge transfer resistance in relation to the interfacial structure.

The equivalent circuit analogous to the interfacial structure for this investigation is illustrated in Figure 8, and the results of the EIS Nyquist plot for each material are shown in Figure 9. All tests followed ASTM G106-89 (2015). In reference to Figure 9:

R_s Solution resistance
R_{ct} Charge transfer resistance of the electron across the metal/electrolyte interface
R_f Film resistance of the oxide film
R_{ad} Resistance as a result of adsorbed corrosion intermediates
Q_f Film capacitance
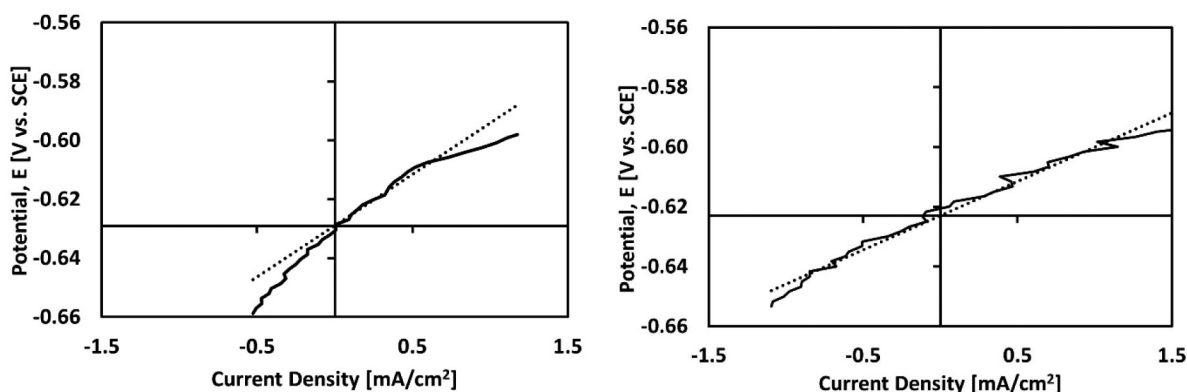Q_{dl} Double layer capacitance
L_{ad} Inductance of adsorbed layer

Figure 7—Average linear polarization resistance for M1 and for M2

Table VI			
Results of LPO analysis and estimated corrosion rate for mesh			
Mesh	**R_p ($\Omega \cdot cm^2$)**	**i_{corr}, R_p (mA/cm^2)**	**Corrosion rate (mm/year)**
M1	32.6±3.8	0.67±0.14	7.89±1.66
M2	22.5±5.6	1.14±0.39	13.19±4.52

Impact of steel properties on the susceptibility to corrosion of weld mesh and mesh straps
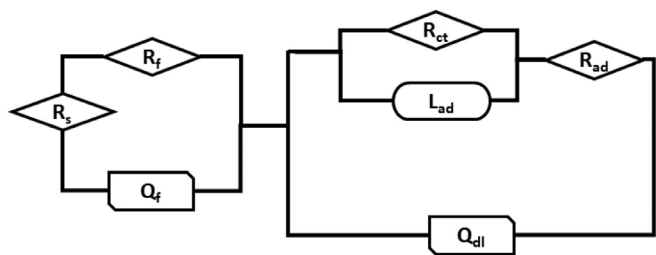

Figure 8—Equivalent circuit used to analyze the impedance response of the material-electrolyte interface for each mesh material
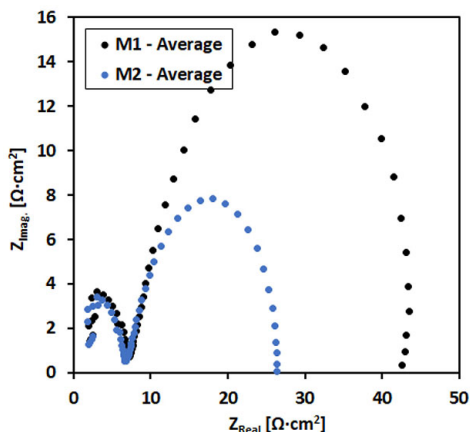

Figure 9—Comparison of EIS for the two mesh samples for 1 h

The resistance data are presented in Figure 10 and summarized in Table VII. In the EIS investigation M2 was more susceptible to corrosion than M1, as indicated by its lower R_{ad} and R_{ct} values. M1 and M2 had similar film resistance values.

The capacitance data are summarized in Figure 11 and Table VIII. Figure 11 illustrates that both mesh materials had similar double layer capacitance values, (Q_{dl}). There was a difference in the value of the film capacitance, (Q_f), indicated in Figure 11 and Table VIII, suggesting the film on M2 might be thicker and porous in nature and hence, less protective than the film formed on M1.
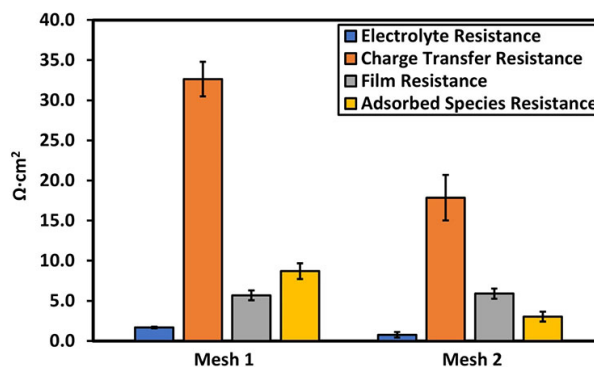

Figure 10—Comparison of electrolyte (R_s), charge transfer (R_{ct}), film (R_f) and adsorbed species resistance (R_{ad})

Table VII				
Resistance data for M1 and M2 mesh				
Mesh	R_s ($\Omega\cdot cm^2$)	R_f ($\Omega\cdot cm^2$)	R_{ad} ($\Omega\cdot cm^2$)	R_{ct} ($\Omega\cdot cm^2$)
M1	1.7 ± 0.1	5.7 ± 0.6	8.7 ± 1.0	32.7 ± 2.1
M2	0.8 ± 0.4	5.9 ± 0.7	3.0 ± 0.6	17.9 ± 2.8

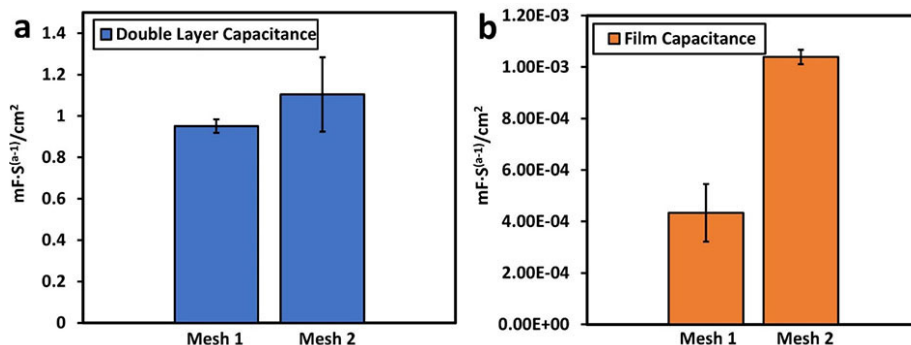| Table VIII		
Comparison of EIS for M1 and M2 mesh samples for 1 h		
Mesh	Q_f (mF s$^{(a-1)}$/cm^2)	Q_{dl} (mF s$^{(a-1)}$/cm^2)
M1	0.0004 ± 0.0001	0.95 ± 0.03
M2	0.0010 ± 0.0000	1.10 ± 0.18

Figure 11—Comparison of double-layer capacitance (Q_{dl}) and film capacitance (Q_f)

Impact of steel properties on the susceptibility to corrosion of weld mesh and mesh straps

Potentiodynamic anodic polarization

Anodic and/or cathodic polarization is a technique wherein the potential of the electrode is varied at a selected rate by the application of a voltage ramp with time and the resultant current is measured. Potentiodynamic anodic polarization (AP) measurements were performed in accordance with ASTM G5 (2014). The results of the potentiodynamic AP analysis for the two meshes (M1 and M2) are presented in Figure 12 and Table IX.

This series of AP tests indicated that the E_{corr} values determined in anodic polarization testing follow the same trend as that observed earlier for OCP measurements, i.e., M2 has a lower value than M1. The corrosion rates of M1 and M2 are statistically very similar but M2 is again slightly more susceptible to corrosion than M1, consistent with the earlier LPR measurements of corrosion rate.

Practical implications for mesh

Based on the relative performance in the undertaken accelerated corrosion tests, the M1 mesh is less susceptible to corrosion than M2 as seen by its higher OCP value, lower i_{corr} in LPR, and higher R_{ct} in EIS. The difference in performance is statistically significant and is attributed to lower carbon and silicon content and slightly higher Ni and Cu content compared to M2. This has significant implications if the mesh is installed in an aggressive corrosion environment. Corrosion of the mesh strands can result in reduced capacity and localized failure that may compromise the integrity of the primary surface support. The implication is that unless the area is rehabilitated, the mesh will be the weak link in the ground support system and can potentially result in a fall of ground.

Accelerated corrosion of mesh straps

The mine was also investigating the corrosion potential of mesh straps when exposed to an aggressive environment. Again, the mesh straps were identified as S1 and S2.

Open-circuit potential (open cell potential)

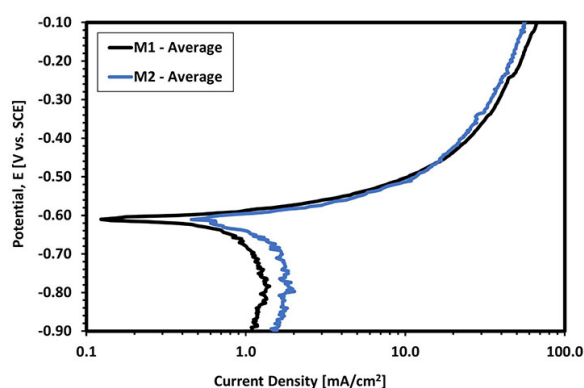The results of the OCP, conducted in accordance with ASTM G5-14,

2014, are summarized in Figure 13 where it can be seen that the OCP of S1 is lower than that of S2 indicating that S1 is more active than S2. An interpretation of the relative performance of the mesh straps is possible by reference to their chemical composition given in Table I.

In general, a higher Mn content should improve corrosion resistance as it decreases the corrosion rate (less negative OCP value). Similarly increased concentrations of C, S, and P content should decrease corrosion resistance, as these elements accelerate the corrosion rate (greater negative OCP value). Finally, the increased Cu and Ni content of S2 relative to S1 should improve the relative corrosion resistance, i.e., it decreases the corrosion rate (lower negative OCP value). In this investigation the higher beneficial Mn content of S1 is offset by the higher C, S, and P content along with lower Cu and Ni concentrations that resulted in the decreased corrosion resistance of S1 relative to S2.

Linear polarization resistance

LPR measurements were performed in accordance with ASTM G59-97 (2014). The results are illustrated in Figure 14. The S2 mesh strap is less susceptible to corrosion than the S1. The linear polarization potential for S2 being R_P = 39.6 $\Omega\cdot cm^2$ compared to R_p = 31.3 $\Omega\cdot cm^2$ for the S1 mesh strap and the corresponding corrosion rates are given in Table X. This agrees with the predicted corrosion behaviour of the OCP values of the two materials, where S2 was predicted to have the lower corrosion rate.

Electrochemical impedance spectroscopy

A series of EIS experiments were performed in accordance with ASTM G106-89 (2015). The same procedure and equivalent circuit analysis (Figure 8) were used as for the mesh. The results of the EIS Nyquist plot for each mesh strap material are shown in Figure 15.

The resistance data are captured in the histogram in Figure 16 and Table XI. In the EIS investigation both mesh strap samples had statistically similar film and charge transfer resistance values. The only significant difference was the resistance of adsorbed species on the surface, with a higher value for the S2 mesh strap compared
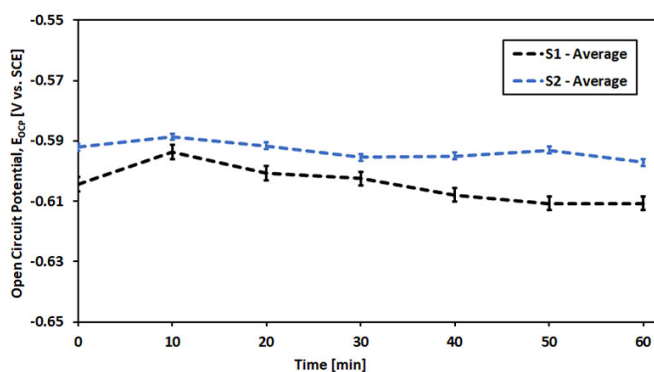
Figure 12—Potentiodynamic polarization using three runs per mesh sample

Figure 13—Open cell potential for mesh straps: S1 -621 mV; S2 -605 mV

Table IX

Potentiodynamic polarization for the mesh samples

Mesh	E_{corr} (V_{SCE})	i_{corr} (mA/cm²)	Corrosion rate (mm/year)	β_a (mV/dec)
M1	-0.610 ± 0.007	1.03 ± 0.09	11.91 ± 1.08	101 ± 11
M2	-0.614 ± 0.010	1.26 ± 0.12	14.62 ± 1.43	112 ± 10

Note: E_{corr}: corrosion potential; i_{corr}: corrosion current density; β_a: anodic Tafel slope
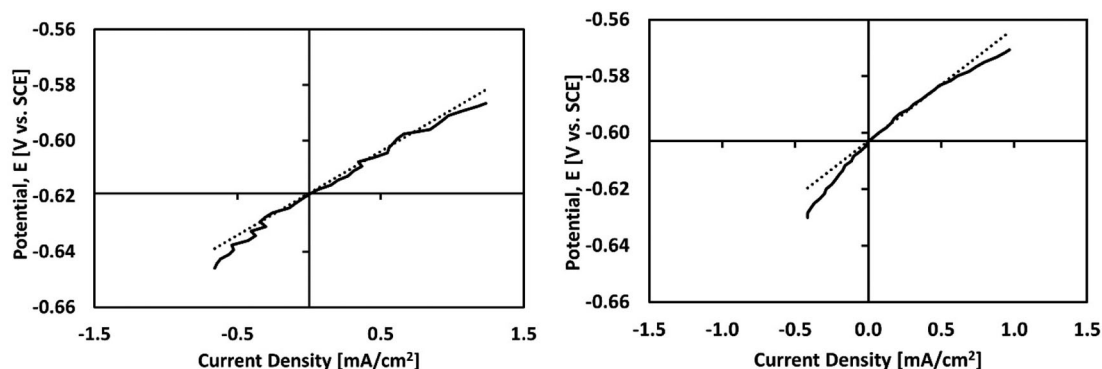
Figure 14—Average linear polarization resistance for S1 and S2 mesh strap

Table X			
Results of LPO analysis and estimated corrosion rate for the mesh straps			
Mesh straps	R_p ($\Omega \cdot cm^2$)	i_{corr}, R_p (mA/cm²)	Corrosion rate (mm/year)
S1	31.3 ± 8.8	0.70 ± 0.15	8.5 ± 1.8
S2	39.6 ± 1.5	0.42 ± 0.01	4.9 ± 02
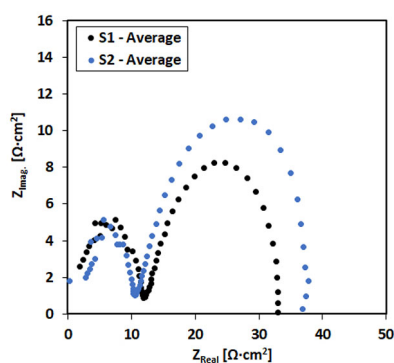
Figure 15—Comparison of EIS for the two mesh strap samples for 1 h

Table XII		
Comparison of EIS for the two mesh strap samples for 1 h		
Mesh strap	Q_f (mF s(a-1)/cm²)	Q_{dl} (mF s(a-1)/cm²)
S1	6.3E-04 ± 5.9E-04	1.1 ± 0.1
S2	1.5E-03 ± 1.3E-04	0.9 ± 0.4

Figure 16—Comparison of electrolyte (R_s), charge transfer (R_{ct}) and film (R_f) resistance for the two mesh straps (S1 and S2)
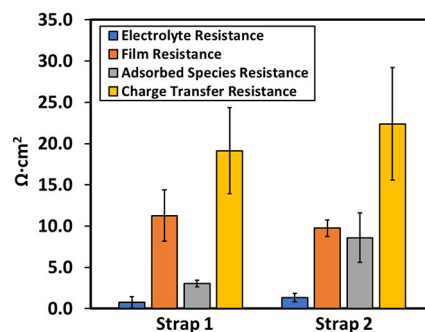
to S1. This is consistent with the trend observed for the mesh samples where the more corrosion resistant material had the higher resistance of adsorbed species.

Figure 17 and Table XII illustrate that both samples had similar double layer capacitance values, (C_{dl}), although there was a clear difference in the film capacitance (Cf). More charge is stored in the surface of the S2 mesh strap, which had better corrosion resistance compared to S1. This is inconsistent with the trend of Cf that was observed for the mesh samples.

Potentiodynamic anodic polarization

Potentiodynamic AP measurements were performed in accordance with ASTM G5 (2014). The results of the potentiodynamic AP analysis for the two mesh straps are presented in Figure 18 and Table XIII.

Practical implications for mesh straps

The provided mesh straps were subjected to a series of accelerated corrosion tests in an aggressive corrosion environment. There was consistent repeatability in the results from all accelerated tests and indicate that the S1 mesh strap was less corrosion resistant than the

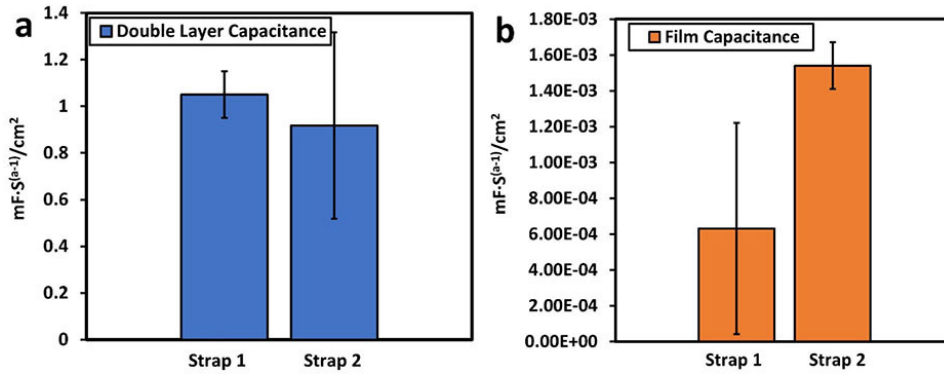| Table XI				
Resistance data for S1 and S2 mesh straps				
Mesh Strap	R_s ($\Omega \cdot cm^2$)	R_f ($\Omega \cdot cm^2$)	R_{ad} ($\Omega \cdot cm^2$)	R_{ct} ($\Omega \cdot cm^2$)
S1	0.8 ± 0.7	11.3 ± 3.1	3.1 ± 0.4	19.1 ± 5.2
S2	1.3 ± 0.5	9.8 ± 1.0	8.6 ± 3.0	22.4 ± 6.8

Figure 17—Comparison of double-layer capacitance (Q_{dl}) and film capacitance (Q_f)
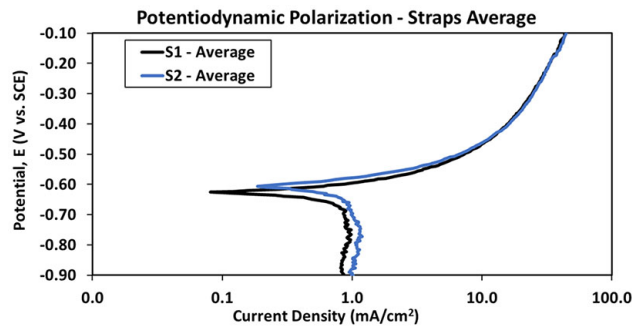

Figure 18—Potentiodynamic polarization using three runs per mesh strap sample

equivalent S2 mesh strap as evident by its more active OCP, and the higher corrosion rate determined in both LPR, and AP testing. This is reflected in the higher corrosion rates.

Conclusions

Primary and secondary surface support are integral parts of a successful ground support system. As part of ground support optimization, it is necessary to explore the use and interaction of different products. The qualification of new products requires a rigorous QA/QC process.

This investigation aimed to identify potential differences in long term performance of steel mesh and mesh straps when exposed to an aggressive environment. Accelerated corrosion techniques were employed to establish a relative ranking of mesh and mesh straps products when exposed to the same aggressive corrosive environment. All tests yielded consistent and repeatable results for both mesh and mesh straps.

The accelerated corrosion studies clearly demonstrated that the difference in performance between the #6 mesh samples from different suppliers was significant. The practical implication is that in an aggressive corrosion environment this will result in a significant reduction in the strand, and consequently, mesh capacity.

A difference in their susceptibility to corrosion was also observed when comparing the S1 and S2 mesh strap samples. The practical implications of this however may not be as significant as for the mesh, as the variations in performance were not as critical. This investigation highlights the need for strict QA/QC on provided ground support elements particularly when comparing elements from different sources. It is also demonstrated that the steel chemistry has a significant impact on the anticipated corrosion when exposed to aggressive environments.

Mesh and mesh straps are only two elements of a ground support system. In practice, failure of any reinforcement or surface support element, can lead to a compromised system. Although degradation in the performance of mesh and mesh straps over time will be dictated by multiple factors, corrosion can be a significant contributing factor. This paper demonstrates that there can be important variations between different mesh and mesh straps products exposed to an aggressive corrosive environment.

Typically, a ground support system will employ mesh as its primary surface support. If higher loads and larger deformations are anticipated, the addition of mesh straps will result in better load distribution and improved performance. The presented accelerated corrosion investigations however identified significant variations

Table XIII

Potentiodynamic polarization for the mesh strap samples

Mesh Strap	E_{corr} (VSCE)	i_{corr} (mA/cm^2)	Corrosion rate (mm/year)	β_a (mV/dec)
S1	-0.626 ± 0.009	0.65 ± 0.04	7.5 ± 0.41	101 ± 4
S2	-0.599 ± 0.008	0.59 ± 0.05	6.81 ± 0.57	77 ± 5

in the long-term performance between mesh and mesh straps. All other factors being equal, the choice of steel for the mesh suggests that in the same environment it would corrode faster than the mesh strap.

The practical implication is that the greater susceptibility to corrosion of mesh compared to mesh straps, is likely to result in earlier failure challenging the integrity of the ground support system. In effect it may be necessary to rehabilitate the primary surface support at an earlier time than the secondary surface support. These should be taken into consideration when determining the true costs of ground support over a longer working life.

Acknowledgements

References

ASTM A1064/A1064M-22. 2022. Standard specification for carbon-steel wire and welded wire reinforcement, plain and deformed, for concrete. *ASTM International*, West Conshohocken, United States

ASTM E18-22. 2022. Standard test methods for Rockwell hardness of metallic materials. *ASTM International*. West Conshohocken, United States.

ASTM E1019-11. 2011. Standard Test Methods for Determination of Carbon, Sulfur, Nitrogen, and Oxygen in Steel, Iron, Nickel, and Cobalt Alloys by Various Combustion and Fusion Techniques. *ASTM International*, West Conshohocken, United States.

ASTM E1479–16. 2016. Standard Practice for Describing and Specifying Inductively Coupled Plasma Atomic Emission Spectrometers. *ASTM International*, West Conshohocken, United States.

ASTM G3-14. 2014. Standard Practice for Conventions Applicable to Electrochemical Measurements in Corrosion Testing. *ASTM International*, West Conshohocken, United States.

ASTM G5–14. 2014. Standard Reference Test Method for Making Potentiodynamic Anodic Polarization Measurements. *ASTM International*, West Conshohocken, United States.

ASTM G59-97. 2014. Standard Test Method for Conducting Potentiodynamic Polarization Resistance Measurements, *ASTM International*, West Conshohocken, PA 19428-2959, United States.

ASTM G106-89. 2015. Standard Practice for Verification of Algorithm and Equipment for Electrochemical Impedance Measurements. *ASTM International*, West Conshohocken, United States.

Baek, B., Karampinos, E., Hadjigeorgiou, J. 2020. Understanding the Impact of Test Configuration on Welded-Wire Mesh Laboratory Test Results. *Rock Mechanics and Rock Engineering*. vol. 53, no. 11, pp. 4873-4892.

Dorion, J.F., Hadjigeorgiou, J. 2014. Corrosion considerations in design and operation of rock support systems. Mining Technology (TIMM A), vol. 23, no. 2, pp. 59–68.

Dorion, J.F., Hadjigeorgiou, J., Ghali, E. 2010. Influence of corrosion rate on the capacity of rock support, ARMA 10-259, American Rock Mechanics Association. *Proceedings 44th US Rock Mechanics Symposium and 5th U.S.-Canada Rock Mechanics Symposium*, 27–30 June 2010, Salt Lake City, UT.

Hadjigeorgiou, J. 2016. Rock support: degradation and failure. *Ground support 2016, the Eighth International Symposium on Ground Support in Mining and Underground Construction*, Luleå, Sweden, E. Nordlund, Jones TH, Eitzenberger A (eds), p. 22.

Hadjigeorgiou, J., Potvin, Y. 2011. Hard Rock Ground Control with Screen and Shotcrete. Chapter 8.6. SME Mining Engineering Handbook. *Society of Mining Engineers*. pp. 573–594.

Hadjigeorgiou, J., Stacey. T.R. 2018. Challenges in determining the capacity of mesh. *AusRock 2018: The Fourth Australasian Ground Control in Mining Conference*, Sydney, NSW, 28–30 November 2018, pp. 280–290.

Hadjigeorgiou, J., Savguira, Y., Thorpe, S.J. 2020. Impact of Steel Properties on the Corrosion of Expandable Rock Bolts. *Rock Mechanics and Rock Engineering*, vol. 53. pp. 705–721.

Hadjigeorgiou, J., Thorpe, S.J., Cole, K.M. 2023. Quality Assurance Considerations for Friction Rock Stabilizers. *Mining Technology (TIMM A)*. vol. 132, no. 1, pp. 17–29.

Hassell, R., Villaescusa, E., Ravikumar, A., Cordova, M. 2010, 'Development of a corrosivity classification for weld mesh support at Cannington Mine', in P Hagan & S Saydam (eds), *Proceedings of the Second Australasian Ground Control in Mining Conference*, The Australasian Institute of Mining and Metallurgy, Melbourne, pp. 1–5.

ISO 18265:2013. 2013. Metallic materials - Conversion of hardness values. Geneva: International Organization for Standardization (ISO).

Player, J.R., Morton, E.C., Thompson, A.G., Villaescusa, E. 2008. Static and dynamic testing of steel wire mesh for mining applications of rock surface support. T.R. Stacey and D. Malan (eds). *Proceedings of the 6th International Symposium on Ground Support in Mining and Civil Engineering Construction*, The South African Institute of Mining and Metallurgy, Johannesburg, pp. 693–706.

Tannant, D. 1995. Load Capacity and Stiffness of Welded-wire Mesh. *Proceedings of the 48th Canadian Geotechnical Conference*. Vancouver, Canada, pp. 729–736.

Wu, S., Northover, M., Craig, P., Canbulat, I., Hagan, P.C., Saydam, S. 2018. Environmental influence on mesh corrosion in underground coal mines. *International Journal of Mining, Reclamation and Environment*, vol. 32, no. 8, 519–535. ◆